高等学校化学学报
CHEMICAL JOURNAL OF CHINESE UNIVERSITIES
研究论文

新型人参多糖的发现: 发酵产物的结构表征、体外发酵特性及其通过Nrf2/HO-1途径对Aβ诱导的PC12细胞的抗氧化机制

董彬彬[1,2], 后　宗[1], 郑　重[1], 邢俊鹏[1], 刘志强[1,2], 刘　舒[1,2]
(1. 中国科学院长春应用化学研究所电分析化学重点实验室&
吉林省中药化学与质谱重点实验室, 长春 130022;
2. 中国科学技术大学应用化学与工程学院, 合肥 230026)

摘要　从人参中分离出一种新型多糖GPA-G2-H, 并对其结构特性、体外酵解特性以及发酵产物FGPA-G2-H对$A\beta_{25\text{-}35}$诱导的PC12细胞的抗氧化机制进行了研究. 通过ζ电位分析、傅里叶变换红外光谱(FTIR)、高效液相色谱(HPLC)、X射线衍射(XRD)、气相色谱-质谱联用(GC-MS)和核磁共振波谱(NMR)等技术对其结构进行了表征. 结果表明, GPA-G2-H的主链主要由→4)-α-D-Glcp-(1→构成, 且支链主要连接于主链的O3位. 体外实验结果表明, GPA-G2-H能够被肠道菌群降解, 这一过程伴随着总糖含量和pH值的降低, 以及短链脂肪酸(SCFAs)含量的增加. 此外, GPA-G2-H可显著促进*Lactobacillus*, *Muribaculaceae*和*Weissella*的增殖, 对肠道菌群的群落组成产生了积极影响. 进一步研究发现, GPA-G2-H的发酵产物FGPA-G2-H能够激活Nrf2/HO-1信号通路, 显著增强HO-1, NQO1, SOD和GSH-Px的活性, 同时抑制Keap1, MDA和LDH的表达, 从而有效缓解Aβ诱导的PC12细胞氧化应激损伤. 研究结果为人参多糖作为功能性食品和抗氧化药物的进一步开发奠定了理论基础.

关键词　人参多糖; 结构表征; 肠道菌群; 发酵性; 氧化应激
中图分类号　O636　　**文献标志码**　A　　doi: 10.7503/cjcu20250314

Discovery of a Novel Ginseng Polysaccharide: Structure Characterization, *in vitro* Fermentability and Anti-oxidative Mechanism of Fermented Product *via* the Nrf2/HO-1 Pathway on Aβ-induced-PC12 Cells

DONG Binbin[1,2], HOU Zong[1], ZHENG Zhong[1], XING Junpeng[1],
LIU Zhiqiang[1,2*], LIU Shu[1,2*]
(*1. Key Laboratory of Electroanalytical Chemistry, Jilin Province Key Laboratory of Chinese Medicine Chemistry and Mass Spectrometry, Changchun Institute of Applied Chemistry, Chinese Academy of Sciences, Changchun* 130022, *China*;
2. School of Applied Chemistry and Engineering, University of Science and Technology of China, Hefei 230026, *China*)

收稿日期: 2025-10-27. 网络首发日期: 2025-11-24.
联系人简介: 刘志强, 男, 博士, 研究员, 主要从事中药药效物质基础方面的研究. E-mail: liuzq@ciac.ac.cn
刘　舒, 女, 博士, 研究员, 主要从事中药药效物质基础方面的研究. E-mail: liushu@ciac.ac.cn
基金项目: 国家重点研究发展计划"中医药现代化"重点专项(批准号: 2023YFC3504000)、吉林省科技发展计划项目(批准号: 20240404043ZP)和长春市"市院科技创新合作专项(批准号: 23SH14)资助.
Supported by the National Key Research and Development Program of Traditional Chinese Medicine Modernization Project, China (No. 2023YFC3504000), the Science and Technology Development Project of Jilin Province, China(No. 20240404043ZP) and the Science and Technology Innovation Cooperation Project of Changchun Science and Technology Bureau and Chinese Academy of Sciences, China(No.23SH14).

Abstract In this study, a novel polysaccharide GPA-G2-H was derived from ginseng. Furthermore, the coherent study of its structural characteristics, fermented characteristics *in vitro*, as well as antioxidant mechanism of fermented product FGPA-G2-H on $A\beta_{25\text{-}35}$-induced PC12 cells were explored. The structure of GPA-G2-H was determined by means of zeta potential analysis, FTIR, HPLC, XRD, GC-MS and NMR. The backbone of GPA-G2-H was mainly composed of →4)-α-D-Glcp-(1→ with branches substituted at O-3. Notably, GPA-G2-H was degraded by intestinal microbiota *in vitro* with total sugar content and pH value decreasing, and short-chain fatty acids(SCFAs) increasing. Moreover, GPA-G2-H significantly promoted the proliferation of *Lactobacillus*, *Muribaculaceae* and *Weissella*, thereby making positive alterations in intestinal microbiota composition. Additionally, FGPA-G2-H activated the Nrf2/HO-1 signaling pathway, enhanced HO-1, NQO1, SOD and GSH-Px, while inhabited Keap1, MDA and LDH, which alleviated Aβ-induced oxidative stress in PC12 cells. These provide a solid theoretical basis for the further development of ginseng polysaccharides as functional food and antioxidant drugs.

Keywords Ginseng polysaccharide; Structural characterization; Intestinal microbiota; Fermentability; Oxidative stress

1 Introduction

Alzheimer's disease(AD) is an age-related neurodegenerative disease characterized by cognitive dysfunction. At present, there are at least 50 million people worldwide suffer from dementia, and with the aging of the population, the incidence of dementia has increased, bringing a huge burden to social medical[1]. The pathologic features of AD include neuronal tangles and amyloid plaque deposition in the brain, which further leads to synaptic loss and neuronal death. The β-amyloid(Aβ) deposition hypothesis has been widely used in the pathogenesis of AD[2]. Moreover, numerous studies have demonstrated evidence that excessive Aβ aggregation elicits neurotoxicity to neurons by the accumulation of oxidative stress, causing apoptosis in neurons, subsequent leading to cognitive impairment[3]. Therefore, it is critical to elucidate the molecular mechanism behind AD, develop effective drugs and reduce the burden of social medical.

Panax ginseng C. A. Meyer belongs to Araliaceae, has been widely used as herbal medicine and functional food. It is recorded in "Sheng Nong's herbal classic" that ginseng has the effect of tranquilizing mind and enhancing intelligence. Ginseng polysaccharides, as natural polymer compounds, are the key active components of ginseng, exhibiting anti-oxidative, anti-inflammatory, immune-regulatory, and neuroprotective effects[4]. In addition, researches have proved that ginseng polysaccharides(GP) could significantly inhibit Aβ deposition, alleviate oxidative stress and neuroinflammation in the brain of AD mice, and improve mitochondrial dysfunction and neuronal loss mitochondrial dysfunction[5]. However, polysaccharides cannot be directly digested and absorbed due to the lack of polysaccharide-degrading enzymes genes in human body. Hence, it is urgent to adopt measures to degrade polysaccharides and improve their activity utilization.

It has been reported that intestinal microbiota contains about 16 carbohydrate esterase families, 22 polysaccharide lyase(PL) families and 130 glycoside hydrolase(GH) families, which enable intestinal microbiota to degrade various polysaccharides[6]. Researches have confirmed that intestinal microbiota could degrade GP to produce the metabolites, which have potential to activate immune active factors in the brain to exert neuroprotective effects[7]. Particularly short-chain fatty acids(SCFAs), the main products of polysaccharide metabolism by the intestinal microbiota, not only provide energy for intestinal epithelial cells but also reduce the growth of pathogenic bacteria and even inhibit glial cell activation and inflammatory responses to alleviate the symptoms of AD patients[8]. Hereby, it is essential to probe the dynamic changes of GP in intestinal microbiota as well as the regulation effects on intestinal microbiota, and investigate the potential mechanisms of the degraded GP on Aβ-induced PC12 cell.

In this study, a novel homogeneous polysaccharide named GPA-G2-H was isolated from GP, the structure was analyzed by means of GPC, zeta potential analysis, FTIR, HPLC, XRD, GC-MS and NMR. Besides, GPA-G2-H was fermented by *in vitro* fermentation model and the changes in its physicochemical properties were detected. The effects of GPA-G2-H on intestinal microbiota were appraised by the changes of microbial community structures and SCFAs contents. Moreover, the fermented GPA-G2-H(FGPA-G2-H) was added to $A\beta_{25\text{-}35}$-induced PC12 cells to investigate its effects on the viability of PC12 cells and anti-oxidative stress ability. Simultaneously, the Nrf2/HO-1 signaling pathway of FGPA-G2-H on PC12 cells was explored. These findings provide a basis for understanding the potential neuroprotective and anti-oxidative stress activity of polysaccharides, and also establish a foundation for the subsequent development of GP in functional foods and antioxidant drugs.

2 Experimental

2.1 Materials and Measurements

P ginseng, Jilin Province, China; *N*-(*tert*-butyldimethylsilyl)-*N*-methyltrifluoroacetamide(MTBSTFA), 99%, Sigma-Aldrich(St Louis, MO, USA); PC12 cells, Shanghai Cell Bank(Shanghai, China); DEAE-cellulose-52 and reducing sugar content assay kit, Solarbio(Beijing, China); 1-phenyl-3-methyl-5-pyrazolinone(PMP), Aladdin(Shanghai, China); 1% penicillin/streptomycin mixture, Biosharp(Beijing, China); The cellular glutathione peroxidase assay kit with NADPH, a total superoxide dismutase(SOD) assay kit with WST-8, lipid peroxidation malondialdehyde(MDA) assay kit and lactate dehydrogenase(LDH) assay kit, Beyotime(Shanghai, China). Enzyme-linked immunosorbent assay(ELISA) kits for tumor necrosis factor(TNF-α), interleukin-1β(IL-1β) and IL-6, MeiKe(Shanghai, China). All other reagents used in this investigation were of analytical purity.

INVENIO-R Fourier transform infrared spectrometer(FTIR), Germany Bruker Company; Agilent 6890-5973 gas chromatography-mass spectrometry system(GC-MS), USA Agilent Technologies Company; Varian BRUKER-500 nuclear magnetic resonance spectrometer(NMR), Germany Bruker Company.

2.2 Preparation of GPA-G2-H

GPA-G2-H was prepared according to the previously reported method with minor adjustments[5]. Briefly, dried ginseng was extracted three times with boiling water(1∶10, *w/v*), concentrated, and subjected to alcoholic precipitation with 80% ethanol, followed removal of protein by the Sevag method to obtain GP. GP was applied to a DEAE-cellulose-52 column (4.0 cm×50 cm), eluted with deionized water and 0.5 mol/L NaCl solution, respectively. The 0.5 mol/L NaCl-eluting fraction was collected and dialyzed to obtain GPA. GPA was further loaded onto a DEAE-cellulose-52 column and sequentially eluted with water, 0.05, 0.1, 0.2, 0.3 mol/L NaCl solution[9]. The third fraction was collected, concentrated, dialysis and purified by 5000 molecular weight ultra-filtered cup to obtain GPA-G2-H.

2.3 Monosaccharide Composition Analysis

The PMP pre-column derivatization method was used to determine the monosaccharide composition of GPA-G2-H[10]. 2 mg of GPA-G2-H were initially hydrolyzed with 0.5 mL of 1 mol/L HCl-MeOH solution at 80 ℃ for 6 h, and repeated three times. The product was further hydrolyzed with 0.5 mL of 2 mol/L trifluoroacetic acid(TFA) at 120 ℃ for 4 h, ethanol was added to remove the excess acid and dried under a nitrogen atmosphere. The hydrolysate was derivatized by 0.5 mol/L PMP and 0.3 mol/L NaOH solution at 80 ℃ for 4 h. Finally, $CHCl_3$ was added to remove the residual PMP, and the filtrate was detected by HPLC with a DAD detector at 245 nm. The mobile phase was composed of 0.05 mol/L PBS solution(B) and acetonitrile(C) and in the volume ratio of 84∶16 at a flow rate of 1.0 mL/min at 30 ℃.

2.4 Determination of Molecular Weight and Zeta Potential

The molecular weight (M_w) of GPA-G2-H was detected by Gel Permeation Chromatography (GPC) on SRT-SEC 100 column, which standard curves were drawn by different molecular weights of dextran (180, 2700, 5250, 9750, 13050, 36800 and 64650 Da). The column was set at 30 ℃ and eluted with anhydrous sodium sulfate solution (0.7%), with a flow rate of 1.0 mL/min. The zeta potential and particle size distribution of GPA-G2-H solution were measured by Nanoparticle analyzer ZS. All samples were prepared into a concentration of 1 mg/mL and performed in triplicate.

2.5 FTIR Analysis

The GPA-G2-H (5 mg) was ground with a spectral-grade KBr powder and pressed into thin sheets. Spectra from 400 cm^{-1} to 4000 cm^{-1} were recorded by a FTIR spectrometer[11].

2.6 Methylation Analysis

The polysaccharide GPA-G2-H was dissolved in anhydrous DMSO, methylated by adding reagents and incubating at 30 ℃ for 60 min, hydrolysis of the methylated polysaccharide with TFA at 120 ℃ for 90 min and reduced with $NaBH_4$ for 8 h. Then the reduced sample was acetylated by adding acetic anhydride for 1 h at 100 ℃. After cooling, toluene was added and concentrated under reduced pressure and evaporated to remove the excess acetic anhydride. The acetylated product was extracted with CH_2Cl_2 for several times, dried with anhydrous sodium sulfate and determined by GC-MS on RXI-5 SIL MS capillary column (30 m×0.25 mm×0.25 mm).

2.7 Nuclear Magnetic Resonance Analysis

GPA-G2-H (40 mg) was dissolved in 0.5 mL of D_2O. The 1D and 2D NMR spectra of GPA-G2-H was recorded by NMR spectrometer.

2.8 Congo Red Test

The conformational structure of GPA-G2-H was analyzed according to Wang method[12]. The polysaccharide GPA-G2-H solution (1.0 mg/mL) and Congo red reagent (80 μmol/L) were mixed at a ratio of 1∶1. The 1 mol/L NaOH solution was added to keep the final concentration of NaOH in the range of 0—0.5 mol/L and maintained for 10 min. The maximum absorption wavelength (λ_{max}) was scanned at 400—600 nm with a spectrophotometer. Deionized water was used instead of polysaccharide solution as a control.

2.9 X-ray Diffraction Analysis

The crystalline structure of GPA-G2-H was measured by a Bruker D8 Advance diffractometer using a Cu $K\alpha$ radiation (λ=1.54 nm) at 40 kV. Scattered radiation was detected by the X-ray diffraction (XRD) in the range of $2\theta = 5^\circ$—80° at a scan rate of 5°/min.

2.10 SEM Analysis

The morphological features of GPA-G2-H was recorded using a scanning electron microscope (SEM). The polysaccharide sample was attached to the conductive adhesive and sputtered using an ion sputtering coating machine. The sample was observed at an accelerated voltage of 5 kV.

2.11 *In Vitro* Fermentation

In vitro fecal fermentation of GPA-G2-H was conducted according to the previously described method with slight modifications[13]. The basal nutrient medium contained 0.10 g NaCl, 0.04 g K_2HPO_4, 0.04 g KH_2PO_4, 2.00 g $NaHCO_3$, 0.25 g resazurin, 2.00 g casein tryptone, 2.00 g yeast extract fermentation, 0.025 g Hemin, 0.50 g *L*-Cysteine hydrochloride, 0.01 g $MgSO_4 \cdot 7H_2O$, 0.01 g $CaC1_2 \cdot 6H_2O$, 2.00 mL Tween 80, 0.50 g bile salts and 2.00 mg Vitamin K1 in 1000 mL of deionized water. The pH value of nutrient medium was adjusted to 7.2 by 0.1 mol/L HCl solution. An amount of fresh feces from 10 healthy rats and 10 $A\beta_{25\text{-}35}$ induced Alzheimer model (AD) rats were collected. The nutrient medium was added and mixed thoroughly to

obtain a fecal solid-liquid mixture(10%, *w*/*v*). 8.0 mL of normal rats' fecal solution supernatant was mixed with 10.0 mL of sterilized fermented medium as a blank control group(the Con group). Then, 8.0 mL of the AD rats' fecal solution supernatant was added to 10.0 mL of sterilized fermented medium as the AD group, and the other added 10.0 mL 9.0 mg/mL of GPA-G2-H dissolved in fermented medium as the GPA-G2-H group respectively. All sealed anaerobic tubes were incubated at 37 ℃ in SCHVTZ Glove anaerobic chamber. The whole process was carried out in an anaerobic system(10%H_2, 5%CO_2 and 85%N_2). The fermented broth was collected after 0, 4, 8, 12, 24, 48 and 72 h and stored at −80 ℃ for further study.

2.12 Determination of Chemical Indices During Fermentation

The fermented products from the Con, AD and GPA-G2-H groups(0, 4, 8, 12, 24, 48 and 72 h) were centrifuged at 5000 r/min for 10 min, then the pH was detected, and the total sugar content was measured *via* the phenol-sulfuric acid method. The reducing sugar content were measured by the reducing sugar content assay kit[14].

2.13 Detection of SCFAs

The SCFAs produced in the Con, AD and GPA-G2-H groups were determined by GC-MS after derivatization with MTBSTFA according to the Xiao method with minor adjustment[15]. The derivatized samples were measured by GC-MS equipped with a TG-5MS(30 m×0.25 mm×0.25 μm) column.

2.14 16S rRNA Gene Sequencing

The 16S rRNA region of the genome was amplified by PCR and the target region DNA was amplified and enriched for high-throughput sequencing. All OTUs were annotated based on the Ribosomal database project (RDP). Results were analyzed in Wekemo Bioincloud(https://www.bioincloud.tech).

2.15 Cell Culture and Model Building

PC12 cells, a neuron-like cell line derived from rat pheochromocytoma, were cultured in DMEM medium containing 1%(volume fraction) penicillin/streptomycin mixture and 10%(volume fraction) fetal bovine serum (FBS). The cells were carried out in incubator containing 5% CO_2 and maintained at 37 ℃. Then PC12 cells were seeded into 96-well plates(4×10^3 cells/well) and cultured for 24 h, injured by $A\beta_{25\text{-}35}$(20 μmol/L) for another 24 h to induce AD-PC12 cells.

2.16 Drug Treatment and Cell Viability

The fermented product of the blank broth(without GPA-G2-H) was boiled in water bath for 15 min, and 95% alcohol was added to broth until alcohol concentration was 80%, and the precipitate and supernatant were collected respectively. The fermented product of the GPA-G2-H group repeated the above operation and collected the precipitate as fermented GPA-G2-H(FGPA-G2-H).

PC12 cells were co-incubated with FGPA-G2-H at different concentrations(0, 31.25, 125, 500, 1000, 2000 and 4000 μg/mL) for 24 h. The (4,5-dimethylthiazol-2-yl)-2,5-diphenyltetrazolium bromide(MTT) assay was used to detect the cell viability and screened the concentration of FGPA-G2-H[16]. The $A\beta_{25\text{-}35}$-induced PC12 cells were incubated with different concentrations of FGPA-G2-H(50, 200 and 800 μg/mL) for 24 h and cell viability was detected by MTT assay.

2.17 Determination of Anti-oxidative Effect of FGPA-G2-H

To study the anti-oxidative effect of FGPA-G2-H on $A\beta_{25\text{-}35}$-induced-PC12 cells, PC12 cells(3×10^5 cells/well) were inoculated into six-well plates and treated according to Section 2.16, the levels of MDA, LDH, GSH-Px and SOD were measured by commercially biochemical kits according to the manufacturer's instructions[17].

2.18 Detection of IL-1β, IL-6 and TNF-α Levels

ELISA measured the concentrations of pro-inflammatory cytokines including the IL-1β, IL-6 and TNF-α

content in cell culture supernatants according to the steps of the manufacturer's instructions[18~20].

2.19 Western Blot

The total protein of each group was extracted by RIPA buffer lysis in ice water bath, and detected by BCA protein assay kit. The protein was separated by SDS-polyacrylamide gel electrophoresis and transferred to the PVDF membrane, and the membrane was blocked with 0.05 g/mL skimmed milk powder TBST solution[21]. PVDF membranes were incubated overnight with NQO1, Keap1, Nrf2, HO-1 and β-actin antibodies at 4 ℃. The membrane was washed three times with TBST and incubated with HRP-conjugated secondary antibody for 1 h. The protein bands were detected using ECL technology. The protein expression was quantitatively analyzed by Image J software.

2.20 Statistical Analysis

All the assays were performed at least in triplicate. The results were expressed as mean±standard deviation(SD). Data were processed using GraphPad Prism and multiple comparisons were performed using one-way analysis of variance(ANOVA). Dunnett's multiple comparison test was employed to evaluate the significance of differences between the groups with different treatments. A P-value<0.05 was considered as statistically significant differences.

3 Results and Discussion

3.1 Monosaccharide Composition and Molecular Weight Analysis

GPA-G2-H was obtained in homogeneous form by subjecting the 0.2 mol/L NaCl-eluted fraction to 5 kDa ultrafiltration according to the fractionation scheme outlined in Section 2.2.(Fig. S1, see the Supporting Information of this paper).

The analytical results of monosaccharide composition showed that GPA-G2-H was composed of galacturonic acid(GalA), glucose(Glc), galactose(Gal), and arabinose(Ara) with a ratio of 1.18∶90.13∶3.74∶4.95[Fig.1(A)]. This indicated that the largest proportion of Glc might be the main skeleton of GPA-G2-H, which was consistent with previous study[7]. The M_w of GPA-G2-H was determined by GPC. The curve of GPA-G2-H showed a single peak[Fig.1(B)], indicating that GPA-G2-H was a homogeneous polysaccharide. The molecular weight of GPA-G2-H was estimated to be 46.29 kDa according to the standard curve of dextran.

3.2 Particle Size Analysis

The size and stability of polysaccharide particles have a great influence on the activity of polysaccharides. In this study, the particle size of GPA-G2-H was found to be (109.69±11.35) nm, which was smaller than GP[Fig.1(C)]. GPA-G2-H with higher absolute value of the negative zeta-potentials might attribute to its GalA and carboxyl groups[22]. The particle surface charge(zeta potential) in polysaccharide solution affects the stability of the dispersion system through electrostatic repulsion(Table 1). The above results demonstrated that GPA-G2-H had a lower molecular size and more negative charges, which was conducive to its stable dispersion in solution.

3.3 FTIR Spectra

The characteristics absorption peak of GPA-G2-H was observed at 400—4000 cm^{-1} as shown in Fig.1(D). The strong and broad peak at 3319 cm^{-1} was assigned to —OH group with stretching, the weak peak around 2916 cm^{-1} corresponded to the stretching vibration of C—H[23]. Besides, the absorption peaks around 1631 cm^{-1} and 1413 cm^{-1} were considered as the vibrations of COO—, indicated the presence of galacturonic acid or glucuronic acid. The signal at 1150—950 cm^{-1} indicated that GPA-G2-H contained pyranose rings, which was attributed to the C—O—C and C—O—H glycosidic bands, and the band at 1074 cm^{-1} contributed to O-substituted glucose residues[24]. Furthermore, absorption at 863 cm^{-1} and 761 cm^{-1} in GPA-G2-H

probably was attributed to the presence of β-type glycosidic bond and furan ring, respectively[25].

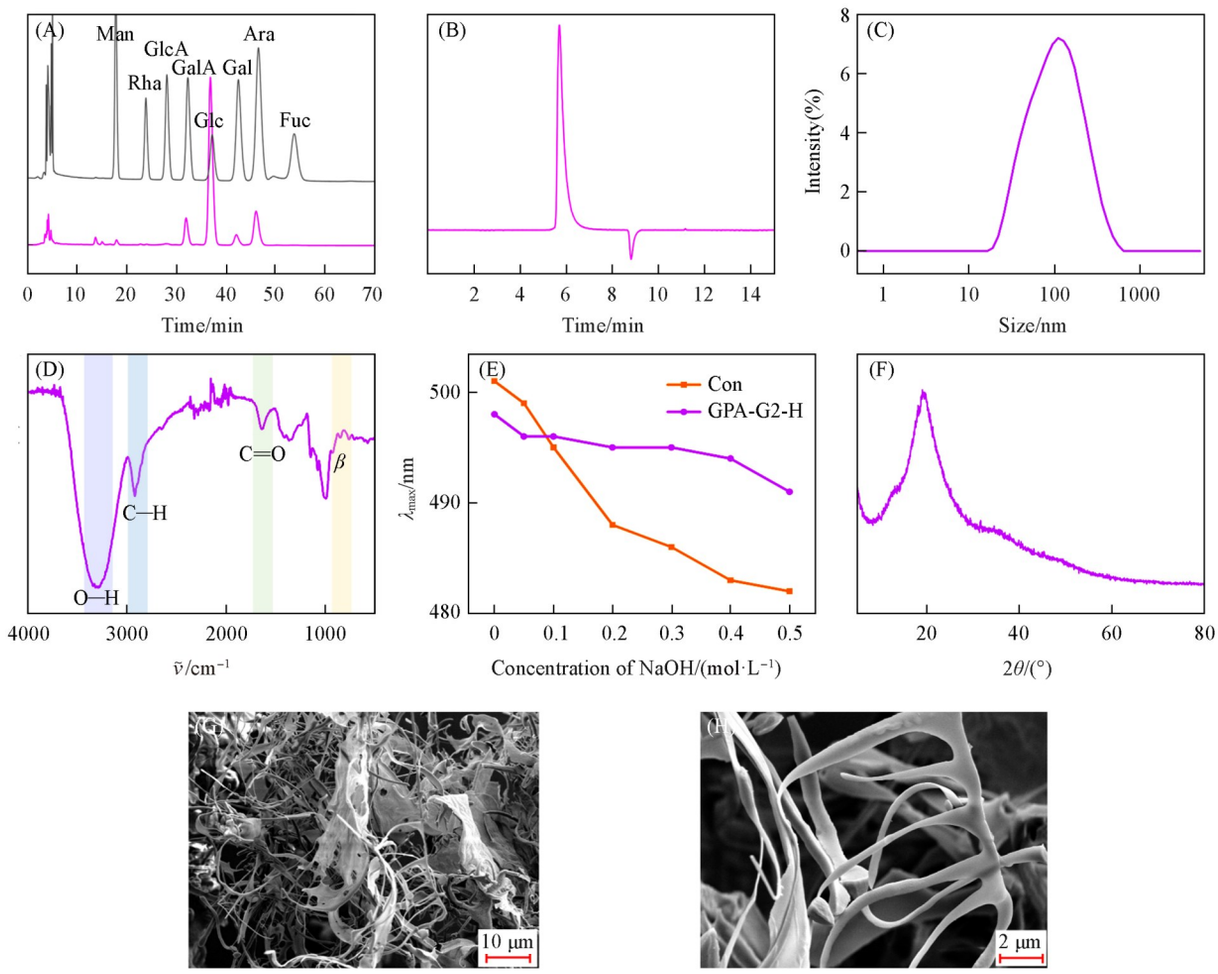

Fig. 1 Physicochemical properties of the polysaccharide GPA-G2-H

(A) HPLC chromatography; (B) GPC profile; (C) molecular particle size distribution; (D) FTIR spectrum; (E) maximum absorption wavelength of Congo red and Congo red+GPA-G2-H at various concentrations of NaOH solution; (F) XRD spectrum; the SEM images of GPA-G2-H with magnifications of 1000×(G) and 5000×(H).

Table 1 Particle size and zeta potential of GPA-G2-H

Sample	Zeta-Average/nm	Zeta-potential/mV
GP	153.30±5.36	−7.94±0.29
GPA-G2-H	109.69±11.35	−11.23±0.37

3.4 Methylation Analysis

To determine the monosaccharide linkages, GPA-G2-H was methylated, hydrolyzed and acetylated for GC-MS analysis. The results of the methylation analysis were summarized in Table 2 and Fig. S2 (see the Supporting Information of this paper), and based on the retention times and standard data of PMAA in the

Table 2 Methylation analysis of GPA-G2-H using GC-MS

RT	PMMA	Type of linkage	Mass fragments, *m/z*	Molar ratio (%)
10.345	2,3,5-Me_3-Araf	Araf-(1→	45,71,87,101,117,129,145,161	1.6
16.845	2,3,4,6-Me_4-Glcp	Glcp-(1→	45,71,87,101,117,129,145,161,205	8.7
21.660	2,3,6-Me_3-Glcp	→4)-Glcp-(1→	45,87,99,101,113,117,129,131,161,173,233	53.6
24.411	2,6-Me_2-Glcp	→3,4)-Glcp-(1→	45,87,97,117,159,185	16.0
26.629	2,3-Me_2-Glcp	→4,6)-Glcp-(1→	45,71,85,87,99,101,117,127,159,161,201,261	7.9

database. The results indicated that GPA-G2-H mainly had five different glycosidic linkages, which were composed of Araf-(1→, Glcp-(1→, →4)-Glcp-(1→, →3, 4)-Glcp-(1→ and →4, 6)-Glcp-(1→ in a molar ratio of 1. 6∶8. 7∶53. 6∶16∶7. 9 and the degree of branching (DB) was 0. 39. The above results indicated that the backbone of GPA-G2-H was probably composed of →4)-Glcp-(1→, and branching at the O3 and O6 positions.

3.5 1D and 2D NMR Analysis

To further analyze the structure of GPA-G2-H, the 1D and 2D NMR spectrum was determined, which was shown in Fig. 2. In ^{1}H NMR spectrum, chemical shifts of the isomeric proton signal greater than δ H5 belong to the α-type and less than 5 for the β-type[26]. The ^{1}H NMR spectrum of GPA-G2-H had multiple strong signals greater than 5, indicating a predominance of α-type chains. The rest signals between δ 3. 48—4. 14 were from H2 to H6.

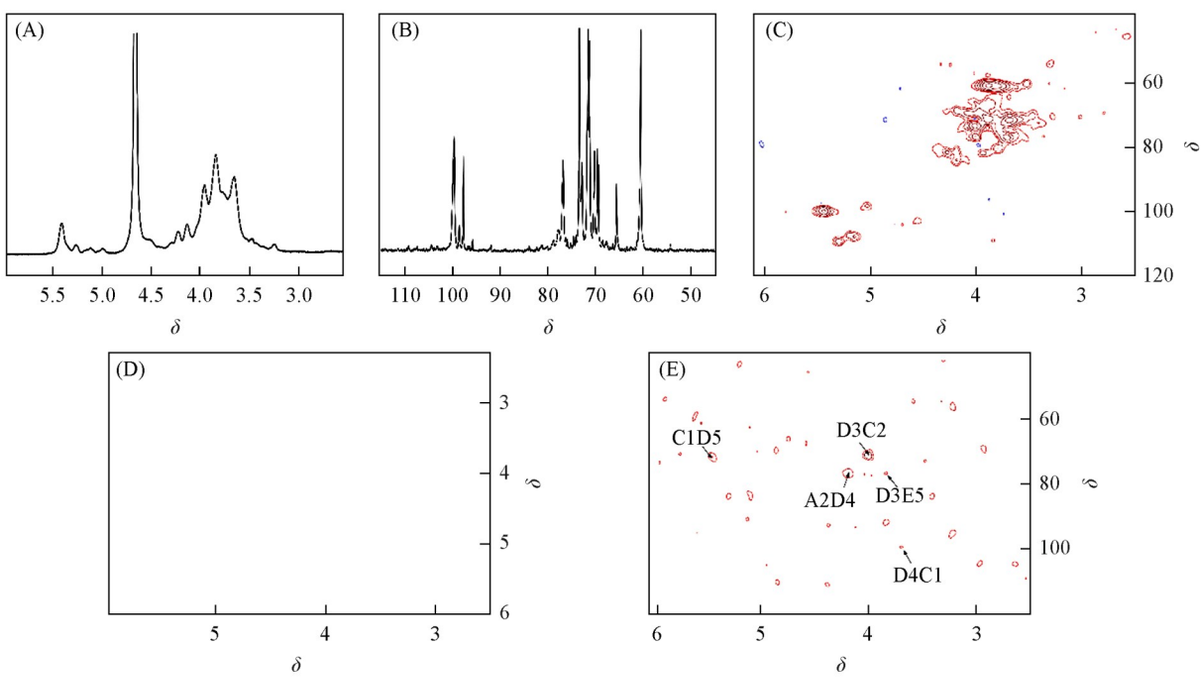

Fig. 2 NMR spectra of the GPA-G2-H

(A) ^{1}H NMR spectrum; (B) ^{13}C NMR spectrum; (C) ^{1}H-^{13}C HSQC spectrum; (D) ^{1}H-^{1}H COSY spectrum in the anomeric region; (E) ^{1}H-^{13}C HMBC spectrum in the anomeric region.

The chemical shifts of C and H in GPA-G2-H were assigned by analysis of HSQC and H-H COSY data [Fig. 2(C) and (D)] regarding literature and methylation results related to the same sugar residues[26~29]. In the anomeric region of the HSQC spectrum, five strong cross peaks were observed at δ 5. 17/108. 93, 5. 03/98. 09, 5. 44/99. 70, 5. 22/107. 43 and 5. 31/109. 82(Table 3), indicating that there were mainly five different sugar residues(A—E). By comparing with methylation and literature, residues A—E were assigned to α-*L*-Araf-(1→, α-*D*-Glcp-(1→, →4)-α-*D*-Glcp-(1→, →3, 4)-α-*D*-Glcp-(1→ and →4, 6)-α-*D*-Glcp-(1→[29,30]. In detail, the correlated HSQC data showed a correlation between the signals of anomeric carbon (δ 199. 70) and anomeric hydrogen(δ 5. 44). The results of further analysis of H-H COSY showed that H1, H2, H3, H4, H5, and H6 were δ 5. 44, 3. 48, 3. 95, 3. 63, 3. 79, and 3. 68, respectively, and the carbon spectra were δ 99. 70, 71. 35, 73. 90, 76. 57, 71. 66 and 61. 43, respectively[31]. The residue was inferred to be glycosidic bond →4)-α-*D*-Glcp-(1→(C). The C and H of the sugar residue *L*-Araf-(1→(A), α-*D*-Glcp-(1→(B), →3,4)-α-*D*-Glcp-(1→(D) and →4,6)-α-*D*-Glcp-(1→(E), were assigned by the same method.

Table 3 Chemical shift of signals of ^{1}H NMR and ^{13}C NMR spectra of GPA-G2-H

	Glycosidic bond	H1/C1	H2/C2	H3/C3	H4/C4	H5/C5	H6/C6
A	α-Araf-(1→	5.17	4.11	4.14	4.10	3.77	—
		108.93	83.13	74.36	83.83	61.21	—
B	α-Glcp-(1→	5.03	3.56	3.70	3.43	3.67	3.65
		98.09	70.95	72.05	69.93	71.43	61.21
C	→4)-α-Glcp-(1→	5.44	3.48	3.95	3.63	3.79	3.68
		99.70	71.35	73.96	76.57	71.66	61.43
D	→3,4)-α-Glcp-(1→	5.22	3.65	3.86	3.59	3.78	3.66
		107.43	72.05	75.68	77.37	70.15	60.90
E	→4,6)-α-Glcp-(1→	5.31	3.57	3.92	3.60	3.77	3.64
		109.82	71.35	75.47	79.42	71.66	64.71

The deduced different sugar residue linkages were further validated by the HMBC. The cross-peaks DH4/CC1 and CH1/DC5 in HMBC spectrum[Fig.2(E)] revealed that C4 of→3,4)-α-*D*-Glcp-(1→ was linked to C1 of →4)-α-*D*-Glcp-(1→, DH3/EC4 and DH3/EC5 indicated that C3 of →3,4)-α-*D*-Glcp-(1→ was linked to C4 of →4,6)-α-*D*-Glcp-(1→[32]. By combination analysis of methylation and NMR spectroscopy, the backbone of GPA-G2-H was mainly composed of →4)-α-*D*-Glcp-(1→ with branches substituted at O3 and terminated with T-α-*D*-Glcp and T-α-*L*-Araf.

3.6 Congo Red Test Analysis

The Congo red test was used to detect whether the polysaccharide had a helical conformation. When the polysaccharide had a triple helix conformation, the λ_{max} of the complex formed by Congo red and polysaccharide will be red-shifted[33]. As shown in Fig.1(E), the λ_{max} of the GPA-G2-H Congo red complex decreased with increasing NaOH concentration, but the decrease trend was slower than that of the Congo red solution. The above results demonstrated that GPA-G-2H had no triple helix structure.

3.7 XRD and SEM Analyses

To further explore the polysaccharide structure, diffraction patterns were obtained by XRD testing of GPA-G2-H. The result showed a broad main diffraction peak at the 2θ of 19.7°[Fig.1(F)], indicating that GPA-G2-H existed mainly in semi-crystalline and amorphous form.

The microscopic surface morphology of GPA-G2-H at different magnifications (1000× and 5000×) was presented in Fig.1(G) and (H). As observed under low magnification, GPA-G2-H was mainly composed of fiber filaments, ribbons with branches and lamellar aggregates, while under high magnification, multiple threads could be seen in a parallel arrangement, suggesting that the chains of GPA-G2-H were arranged in a somewhat ordered manner.

3.8 Changes of pH, Total Sugar and Reducing Sugar During Fermentation

The changes of total sugar content can provide evidence for the utilization and degradation of polysaccharides by the intestinal microbiota. The total sugar content of GPA-G2-H group decreased from 2.76 to 1.15 mg/mL within 24 h[Fig.3(A)], which was significantly higher compared to the Con and AD groups (P<0.05). The result demonstrated the majority of the GPA-G2-H could be utilized by the intestinal microbiota.

In addition, the polysaccharide can be degraded by the enzyme secreted by the intestinal microbiota, with more reducing ends exposing. The GPA-G2-H group decreased significantly (P<0.05) in reducing sugar content before an initial increase at 8 h[Fig.3(B)], The results were consistent with the results of other polysaccharides fermented *in vitro*[6]. This could be explained by the fact that within the first 8 h, the rate at which polysaccharides were utilized was outpaced by the intestinal microbiota's capacity to hydrolyze them. However, after this period, the condition reversed as a result of the intestinal microbiota's higher metabolism brought on by their multiplication.

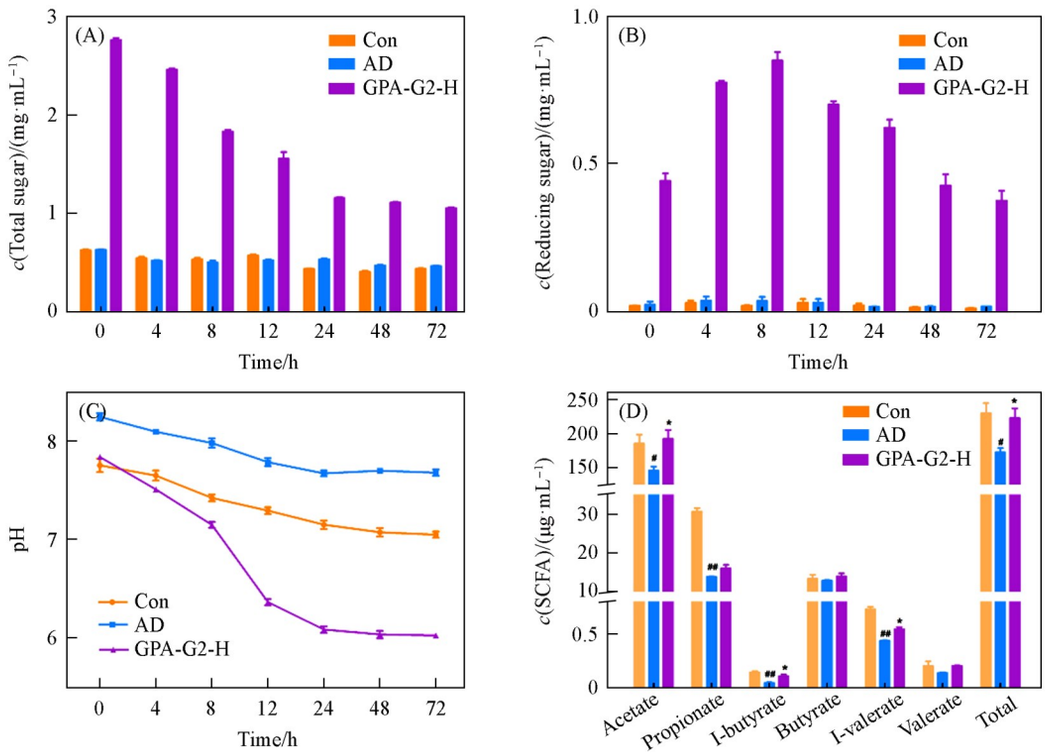

Fig. 3 Total sugar concentration changes(A), reducing sugar content changes(B), the pH changes of GPA-G2-H during *in vitro* digestion(C) and concentrations of SCFAs(D)

Data were expressed as means±SD(n = 3); $^{\#}P$<0.05, $^{\#\#}P$<0.01 *vs.* Con group, *P<0.05 *vs.* AD group.

The change of pH in fermented broth reflected the change of GPA-G2-H metabolism during fermentation process in a certain extent. As shown in Fig.3(C), the initial pH of GPA-G2-H fermentation was significantly lower than that of the AD group, which might be related to the GalA content in GPA-G2-H[34]. GPA-G2-H had a slower decreasing trend before 8 h, while the decreasing effect was very obvious from 8 to 24 h, which might be due to the proliferation of intestinal microbiota. In addition, the rise in the degradation and utilization rate of GPA-G2-H led to an increase in acid metabolites and a decrease in pH.

3.9 SCFAs Levels

Studies have shown that intestinal microbiota is closely related to human health, and SCFAs are the main metabolites of polysaccharides utilization by intestinal microorganisms and have a regulatory effect on the microbiota[35]. The content of SCFAs in each fermentation group was shown in Fig.3(D). The concentration of acetic acid, propionic acid, and isovaleric acid in the AD group was significantly lower than that in the Con group. When treated with GPA-G2-H, the concentration of acetic acid, isobutyric acid, and isovaleric acid increased significantly. This increase might be attributed to the GPA-G2-H promoted the proliferation and metabolism of beneficial bacteria. As the growth substrate of intestinal microbiota, GPA-G2-H provides energy for the reproduction of intestinal microbiota. In previous research, the metabolically produced SCFAs could be absorbed by the colonic epithelium and transported to organs and target tissues, activated immune-active cells in the brain and provided energy for heart, brain, nerve tissue *etc.*[36], and inhibited reproduction of pathogenic bacteria to alleviate the symptoms of the host. Therefore, these results inferred that GPA-G2-H might improve the intestinal microenvironment by producing SCFAs and remodeling the structure of the intestinal microbiota to improve the host AD symptoms. To further validated the above conjecture, we sequenced the 16S rRNA of fecal ferment.

3.10 Composition of Intestinal Microbiota

The regulation effect of GPA-G2-H on the composition of intestinal microbiota was investigated by 16S rRNA sequencing. At the genus level [Fig. 4(A)], statistically significant decreases in *Lactobacillus*, *Muribaculaceae* and *Weissella*, while increases in *Blautia* and *Fusicatenibacter* were seen in AD group as compared to Con group (P<0. 05). The supplement of GPA-G2-H as a carbon source significantly decreased the abundance of *Blautia* and *Fusicatenibacter*, while greatly increased *Lactobacillus*, *Muribaculaceae* and *Weissella* comparing with AD group. *Lactobacillus* is a probiotic, researches have shown the supernatant of *Lactobacillus* could reverse oxidative stress and inflammatory response in the hippocampus to improve cognitive impairment and exert neuroprotective effects[37], *Muribaculaceae*, as the dominant family of the *Bacteroidaceae*, encodes a large number of enzymes that hydrolyze carbohydrates, thus possessing a strong ability to metabolize both endogenous and exogenous polysaccharides[38]. GPA-G2-H was used as the energy source for *Muribaculaceae*, promoted its proliferation in the intestine, and produced SCFAs. Besides, *Muribaculaceae* could accelerate the rate of SCFAs production by cross-feeding with *Lactobacillus* and *Bifidobacterium*.

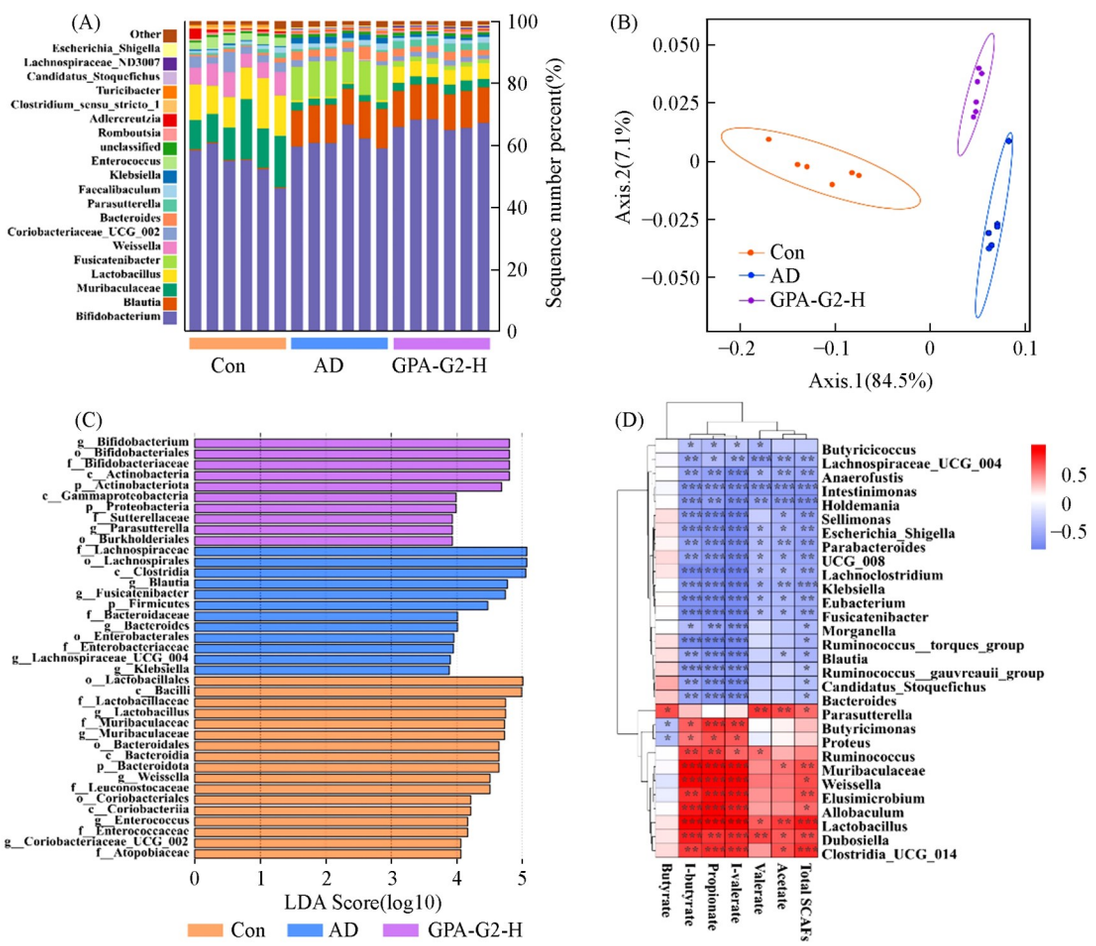

Fig. 4 Effect of GPA-G2-H on intestinal microbiota

(A) relative abundance at genus level; (B) PCoA based on Bray-Curtis distances; (C) LDA scores with corresponding phylum; (D) correlation between and SCFAs content and the abundance of microbiota at the phylum level. Data were expressed as means ± SD (n = 6), *P < 0. 05, **P < 0. 01, ***P < 0. 001 *vs*. AD group.

Principal coordinate analysis (PCoA) is a non-binding data dimension reduction analysis method and was used to visually analyze the overall differences in the intestinal microbiota between different groups. The more similar the composition of the intestinal microbiota, the closer they were on the PCoA map. The Con, AD,

and GPA-G2-H groups were significantly separated from each other on the PCoA plots, which suggested that there was a significant difference in intestinal microbiota composition between these groups[Fig.4(B)]. The microbiota composition was obviously away from the AD group and closer to Con group on the PCoA plot under the treatment of GPA-G2-H, suggesting that GPA-G2-H had a retrogressive effect on the microbial community.

Linear discriminant analysis (LDA) is a classical classification model that identifies genomic features characterizing differences between two or more biological conditions. As shown in Fig.4(C), the 39 genera with LDA scores of 4.0 or more showed significant differences among all groups. The dominant genera in the Con, AD, and GPA-G2-H groups were 10, 12, and 17 species, respectively. Especially, *Bacteroides* and *Klebsiella* were found in AD group as the dominant species, which had recently been demonstrated to be capable of forming extracellular amyloids and were associated with inflammation[39]. *Bifidobacterium* and *Actinobacteriota* were the dominant species in the GPA-G2-H group. It had reported that *Bifidobacterium* regulated amino acid metabolism to improve cognitive impairment and alleviate Alzheimer's disease[40]. Kim *et al.*[41] found that *Bifidobacterium* effectively inhibited amyloidosis and improved synaptic plasticity by ameliorating neuroinflammatory responses. The result indicated that the supplement of GPA-G2-H had potential to modulate the microbial composition of the AD.

To further explore the relationship between intestinal microbiota and metabolic changes, a Spearman correlation analysis was conducted between differential bacteria and SCFAs. The result was depicted in the form of heatmap in Fig.4(D). The relative abundance of the genera *Butyricimonas*, *Lactobacillus*, *Paraprevotella*, *Muribaculaceae* and *Weissella* were positively correlated with SCFAs, especially stronger correlated with propionic acid and butyric acid. Besides, *Eubacterium*, *Klebsiella* and *Bacteroides* were negatively correlated with acetic acid, propionic acid and butyric acid. The above results revealed the relationship between specific intestinal microbiota and SCFAs, and provided a basis for further research into the GPA-G2-H-mediated modulation on intestinal microbiota.

Numerous studies have confirmed that polysaccharides serve as effective prebiotics that can regulate specific bacterial strains and significantly promote human health[42]. With the intervention of GPA-G2-H, the abundance of *Lactobacillus* and *Muribaculaceae* increased significantly in the fermentation community. *Lactobacillus* is a probiotic, researches have shown the supernatant of *Lactobacillus* could reverse oxidative stress and inflammatory response in the hippocampus to improve cognitive impairment and exert neuroprotective effects[37]. *Muribaculaceae*, as the dominant family of the *Bacteroidaceae*, encodes a large number of enzymes that hydrolyze carbohydrates, thus possessing a strong ability to metabolize both endogenous and exogenous polysaccharides[38]. Besides, *Muribaculaceae* could accelerate the rate of SCFAs production by cross-feeding with *Lactobacillus* and *Bifidobacterium*. Notably, *Bifidobacterium* emerged as a dominant bacterial in the GPA-G2-H group. Researches indicate that *Bifidobacterium* is an important acid-producing probiotic, capable of synthesizing SCFAs such as acetic acid, propionic acid, and lactic acid.

SCFAs play crucial roles in maintaining the balance of intestinal microbiota and supporting overall metabolic health. Acetic acid was the main fermentation products in the intestinal microbiota after GPA-G2-H intervention, which was consistent with previous studies[43]. It has reported that acetic acid could reduce the intestinal pH to inhibit the growth of pathogenic bacteria. In addition, acetic acid promotes the proliferation of beneficial bacteria such as *Bifidobacterium* and *Lactobacillus* through multiple mechanisms, including regulating intestinal pH, serving as an energy source, and promoting cross-feeding interactions, thereby maintaining the balance of intestinal microbiota[44]. The increased abundance of *Bifidobacterium* and *Lactobacillus* after GPA-G2-H intervention in this study might be related to its production of acetic acid. In general, these findings indicate that GPA-G2-H promoted the production of SCFAs and regulated the homeostasis of intestinal microbiota

to exert potential probiotic functions.

3.11 Effect of FGPA-G2-H on A$\beta_{25\text{-}35}$-induced PC12

3.11.1 Effect of FGPA-G2-H on Viability of A$\beta_{25\text{-}35}$-induced PC12 Cells To explore the appropriate concentration of FGPA-G2-H, PC12 cells were treated with various FGPA-G2-H concentrations for 24 h. The MTT assay (Fig.S3, see the Supporting Information of this paper) showed that FGPA-G2-H had no inhibition and toxicity to the PC12 cells when the concentration below 1000 μg/mL. Therefore, less than 1000 μg/mL FGPA-G2-H was used for subsequent studies. The effect of various concentrations FGPA-G2-H(50, 200, 800 μg/mL) on A$\beta_{25\text{-}35}$-induced PC12 cells were further detected by MTT assay and the result showed in Fig.5(A). Under treatment with different concentrations of FGPA-G2-H, the viability of PC12 cells was improved in a dose-dependent manner and enhanced to 75.25% when cells were treated with 800 μg/mL FGPA-G2-H, which was significantly (P<0.05) higher than AD group cells. The result indicated that FGPA-G2-H had a protective effect on A$\beta_{25\text{-}35}$-induced damage to PC12 cells.

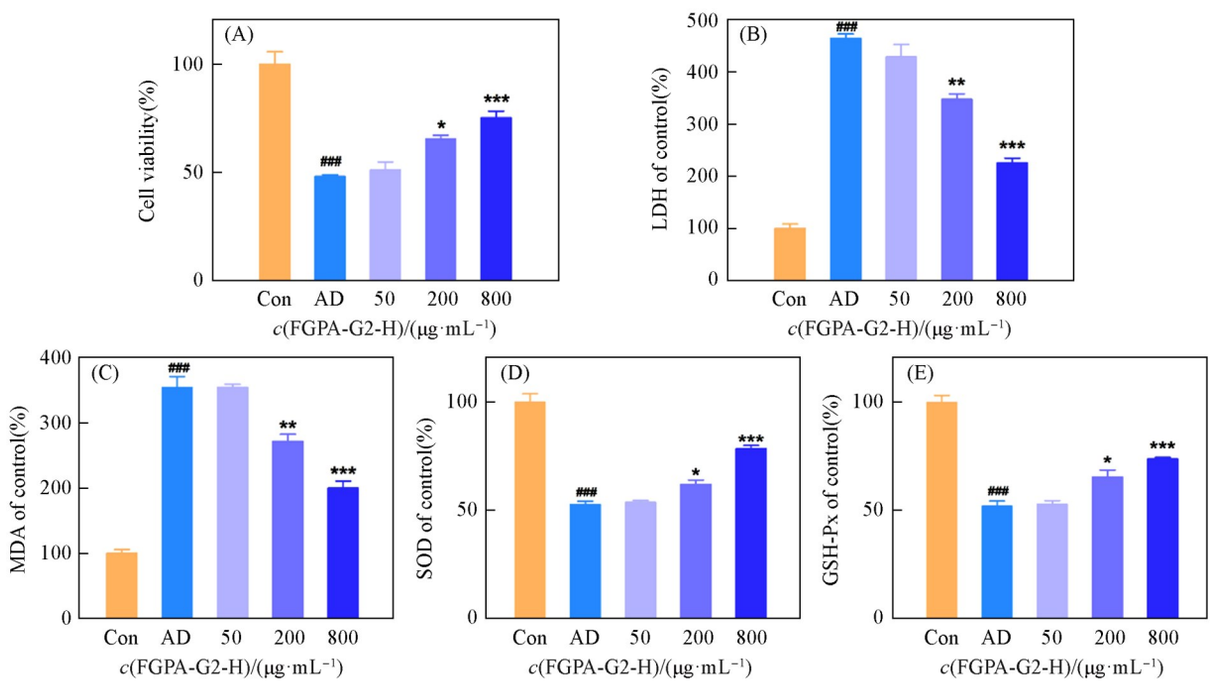

Fig. 5 Effect of FGPA-G2-H(50, 200, 800 μg/mL) on the A$\beta_{25\text{-}35}$ injured PC12 cells viability(A), levels of LDH(B), MDA(C), SOD(D), GSH-Px(E) in A$\beta_{25\text{-}35}$ injured PC12 cells

Data were expressed as mean±SD(n=4). Differences are statistically significant at $^{###}P$<0.001 *vs*. Con group without A$\beta_{25\text{-}35}$, $^{*}P$<0.05, $^{**}P$<0.01 *vs*. AD group treated with A$\beta_{25\text{-}35}$ alone.

3.11.2 Anti-oxidative Effect of FGPA-G2-H on A$\beta_{25\text{-}35}$-induced PC12 Cells To further investigated the effect of GPA-G2-H on oxidative stress, the MDA, SOD, GSH-Px and LDH in A$\beta_{25\text{-}35}$-induced cells under FGPA-G2-H administration were measured. LDH is one of the key oxidoreductases in organisms, which can reflect the active state of cells. When cells are damaged, the permeability of cell membrane increases, and LDH is released from the cell into the culture medium[45]. LDH in the AD group increased after treatment with 20 μmol/L A$\beta_{25\text{-}35}$ for 24 h, suggesting that A$\beta_{25\text{-}35}$ significantly increased cell membrane permeability and induced the release of LDH[Fig.5(B)]. Administrating with 800 μg/mL of FGPA-G2-H, LDH significantly decreased to 225.78% (P<0.01). Meanwhile, FGPA-G2-H significantly reduced MDA in a dose-dependent manner [Fig.5(C)], suggesting that GPA-G2-H maintained normal metabolic activities of PC12 cells by enhancing cell membrane integrity and reducing MDA accumulation.

SOD and GSH-Px can scavenge peroxides in living cells and protect cells from radical damage. As

compared to the Con group, the activities of SOD and GSH-Px in the AD group were decreased, while treatment with different concentrations of FGPA-G2-H enhanced the activities of SOD and GSH-Px[Fig.5(D) and (E)]. SOD and GSH-Px play crucial roles in the reduction and detoxification of peroxides. With the increase of GSH-Px and SOD activity, free radicals in cells were effectively eliminated and oxidative damage was reduced[46]. The results demonstrated that FGPA-G2-H significantly increased GSH-Px and SOD synthesis in the high-dose group and reduced A$\beta_{25\text{-}35}$-induced cytotoxicity. Based on these findings, FGPA-G2-H appeared to have protective effects against oxidative damage caused by A$\beta_{25\text{-}35}$.

3.11.3 Inflammation Effect of FGPA-G2-H on A$\beta_{25\text{-}35}$-induced PC12 Cells Previous studies have demonstrated that Aβ protein promotes AD disease progression and localized neuroinflammatory activity[47]. Therefore, the effect of FGPA-G2-H on neuroinflammatory activity in A$\beta_{25\text{-}35}$-induced PC12 cells was also examined. A$\beta_{25\text{-}35}$ caused a significant increase in the levels of pro-inflammatory cytokines released by PC12 cells, including IL-1β, IL-6 and TNF-α(Fig.6). FGPA-G2-H significantly reduced the levels of pro-inflammatory cytokines in a concentration-dependent manner, IL-1β, IL-6, and TNF-α were reduced to 10.06%, 47.69%, and 48.32% of those in the AD group respectively. Yang *et al.*[48] confirmed that a plant active polysaccharide from *Nicotiana* improves lead-induced inflammation and spatial memory impairment in mice by regulating IL-6. Collectively, these results suggested that FGPA-G2-H could exert neuroprotective effects by inhibiting the expression of proinflammatory cytokines induced by A$\beta_{25\text{-}35}$.

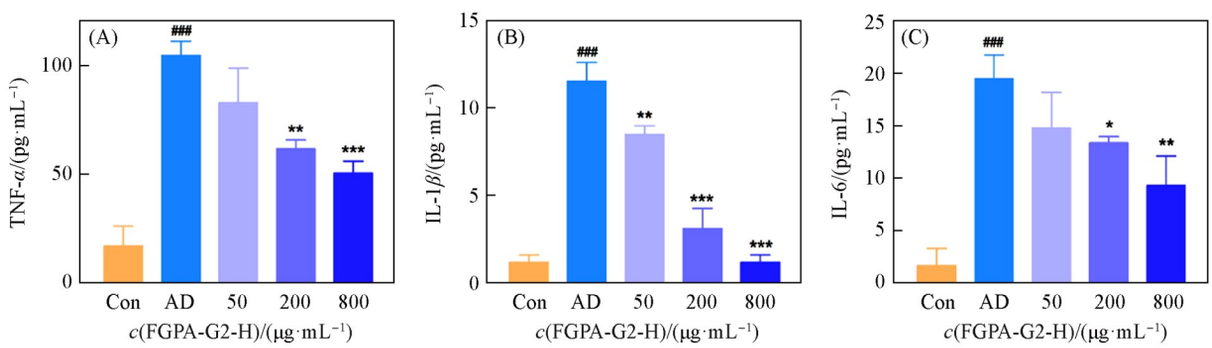

Fig. 6 Effect of FGPA-G2-H(50, 200, 800 μg/mL) onTNF-α(A), IL-1β(B) and IL-6(C) content in A$\beta_{25\text{-}35}$-induced PC12 cells

Data were expressed as mean±SD(n=4). Differences are statistically significant at $^{###}P$<0.001 *vs.* Con group without A$\beta_{25\text{-}35}$, $^{*}P$<0.05, $^{**}P$<0.01 *vs.* AD group treated with A$\beta_{25\text{-}35}$ alone.

3.11.4 Effect of FGPA-G2-H on the Expression of Nrf2/HO-1 Signaling in A$\beta_{25\text{-}35}$-Induced PC12 cells Nrf2/HO-1 pathway is considered to be a pivotal antioxidant pathway for cells in response to oxidative damage. Nrf2, a crucial regulator in the Nrf2/HO-1 signaling pathway, could release from Kelch-like ECH-associated protein 1 (Keap1) once activated, and translocate to the nucleus, further activating the expression of downstream antioxidant, such as heme oxygenase1(HO-1), quinone oxidoreductase 1(NQO1), SOD and GSH-Px. HO-1 and NQO1 are critical mediators of cellular protection against oxidative stress, maintaining redox homeostasis during exposure to nerve injury[49]. To assess the effect of FGPA-G2-H on Nrf2/HO-1 signaling pathway, the gene expression of Nrf2, HO-1, NQO1 and Keap1 in PC12 cells was detected. Western blot results(Fig.7) showed that compared with Con group, expression of Nrf2, NQO1 and HO-1 in PC12 cells induced with A$\beta_{25\text{-}35}$(AD group) was significant downregulated(P<0.01). By contrast, the expressions of Nrf2, NQO1, and HO-1 were elevated, while the protein expression of Keap1 was downregulated under the intervention of 800 μg/mL FGPA-G2-H. Meng *et al.*[50] found that *Salvia miltiorrhiza* polysaccharides(SMPs) activated Nrf2/HO-1 pathway to increase SOD and GSH-Px activities, further prevented lipid peroxidation and apoptosis of PC12 cells. Collectively, the results suggested that Nrf2 activation was a key mechanism in

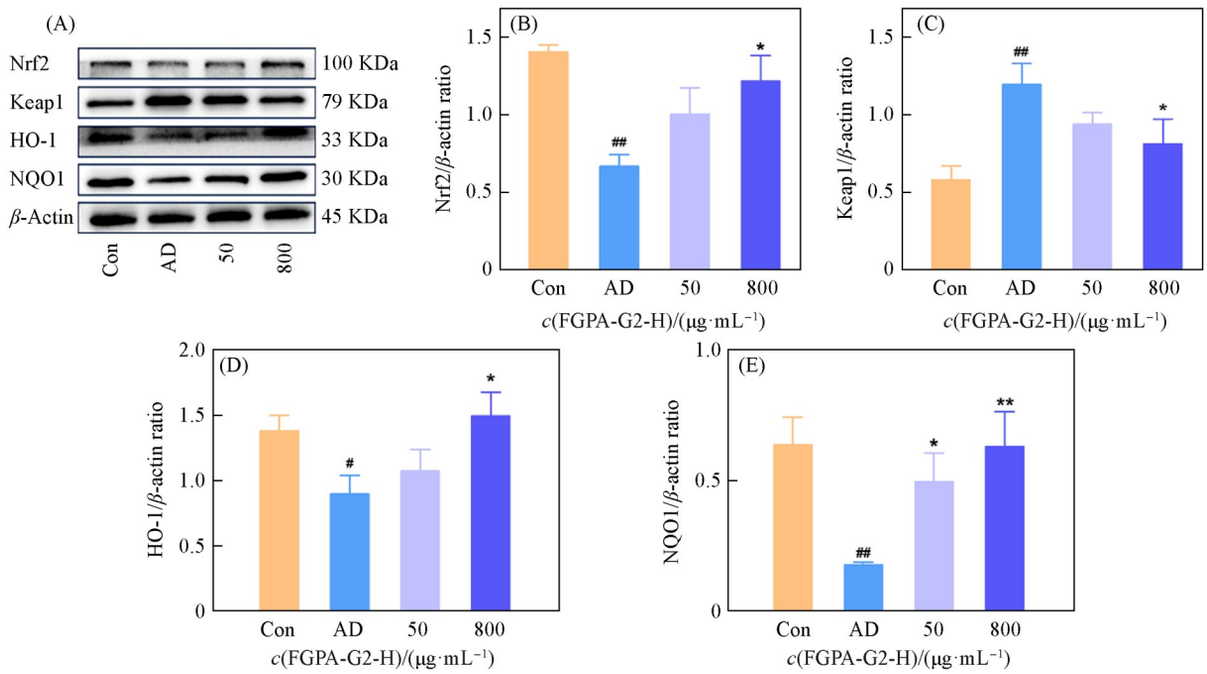

Fig. 7　FGPA-G2-H activated Nrf2 pathway-related protein expression in Aβ_{25-35}-induced PC12 cells

(A) Western blot assay of Nrf2, Keap1, HO-1 and NQO1, the relative ratio of Nrf2(B), Keap1(C), HO-1(D), and NQO1 proteins(F) was quantified. β-actin served as the internal reference. Data were expressed as mean±SD(n=3). Differences are statistically significant at # P<0.01, ## P<0.01 *vs.* Con group without Aβ_{25-35}, *P<0.05, **P<0.01 *vs.* AD group treated with Aβ_{25-35} alone.

FGPA-G2-H alleviating Aβ_{25-35}-induced damage in PC12 cells, and the proposed pathway illustration was presented in Fig.8.

Part A: the mechanism of Aβ_{25-35}-induced PC12 cellular model of AD involving Nrf2/HO-1 signaling pathway and oxidative stress; part B: the protective activity of FGPA-G2-H treatment in Aβ_{25-35}-induced PC12 cellular model of AD.

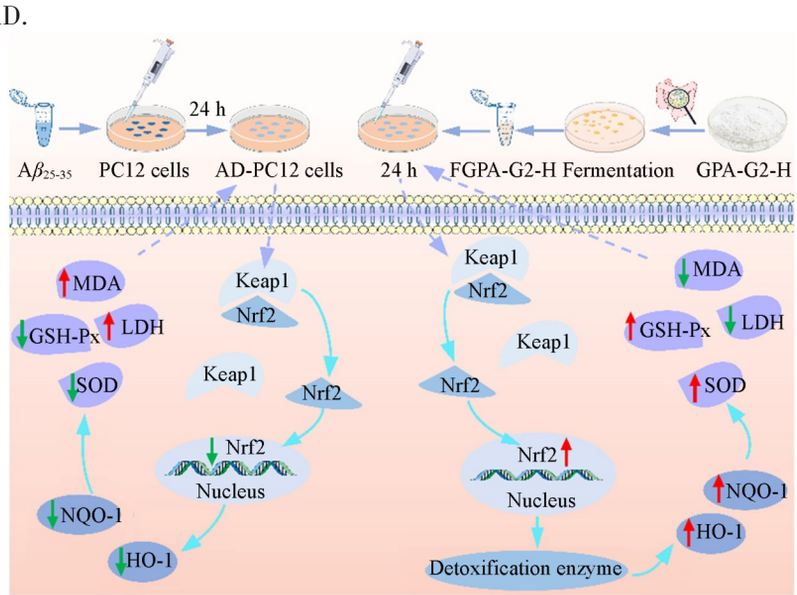

Fig. 8　Pathway illustration of the protective activity of FGPA-G2-H treatment in Aβ_{25-35}-induced PC12 cell injury

4　Conclusions

In conclusion, a novel homogeneous polysaccharide GPA-G2-H derived from ginseng had excellent

probiotic properties and its fermented product FGPA-G2-H alleviated oxidative stress on A$\beta_{25\text{-}35}$-induced PC12 cells. The backbone of GPA-G2-H was mainly composed of →4)-α-D-Glcp-(1→ with branches substituted at O3. GPA-G2-H reshaped the composition of the intestinal microbiota by promoting the proliferation of beneficial bacteria such as *Lactobacillus*, *Muribaculaceae* and *Weissella*, while inhibiting the proliferation of pathogenic bacteria, as well as promoting the synthesis of SCFAs. Additionally, it was demonstrated that GPA-G2-H could be fully metabolized by the intestinal microbiota and the metabolized product FGPA-G2-H exerted the potential neuroprotective activity against oxidative stress in PC12 cells induced by A$\beta_{25\text{-}35}$ through attenuating proinflammatory cytokines (TNF-α, IL-1β and IL-6) generation, MDA accumulation, and promoting SOD and GSH-Px synthesis. Moreover, FGPA-G2-H probably prevented A$\beta_{25\text{-}35}$-induced oxidative injury in PC12 cells by regulating Nrf2/HO-1 signaling pathway. Hence, GPA-G2-H is a potential neuroprotective and antioxidant polysaccharide, and further *in vivo* studies are needed in the future. The study might facilitate understanding the biological functions of GP, and lay foundation for the subsequent development of GP as functional food and oxidant drugs.

The Supporting Information of this paper see http://www.cjcu.jlu.edu.cn/CN/10.7503/cjcu20250314.

References

[1] Fu J., Li J. X., Sun Y. Z., Liu S., Song F. R., Liu Z. Y., *Int. J. Biol. Macromol.*, **2023**, *232*, 123488
[2] Bian Z. Y., Cao C. Z., Ding J., Ding L., Yu S., Zhang C. X., Liu Q., Zhu L. H., Li J., Zhang Y. Q., Liu Y. H., *J. Ethnopharmacol.*, **2023**, *313*, 116550
[3] Zhang R. L., Lei B. X., Wu G. Y., Wang Y. Y., Huang Q. H., *Bioorg. Chem.*, **2023**, *133*, 106210
[4] Wang N., Wang X. L., He M. J., Zheng W. X., Qi D. M., Zhang Y. Q., Han C. C., *J. Ginseng Res.*, **2021**, *45*(2), 211—217
[5] Zhang S., Liu F. B., Li J. M., Jing C. X., Lu J., Chen X. N., Wang D. D., Cao D. H., Zhao D. Q., Sun L. W., *Biomed. Pharmacother.*, **2023**, *167*, 115442
[6] Wang Q. Q., Chen H. M., Yin M. Z., Cheng X., Xia H., Hu H. M., Zheng J. P., Zhang Z. G., Liu H., *Front. Cell. Infect. Mi.*, **2023**, *13*, 1105335
[7] Wang D. D., Shao S., Zhang Y. Q., Zhao D. Q., Wang M. X., *Front. Immunol.*, **2021**, *12*, 683911
[8] Sun Y., Zhang H. W., Zhang X., Wang W. Z., Chen Y., Cai Z. Y., Wang Q. H., Wang J., Shi Y., *Redox Biol.*, **2023**, *62*, 102690
[9] Zhang H., Zou P., Zhao H. T., Qiu J. Q., Mac Regenstein J. , Yang X., *Carbohyd. Polym.*, **2021**, *251*, 117078
[10] Qi Z. H., Gao T. X., Li J. J., Zhou S. H., Zhang Z. G., Yin M. Z., Hu H. M., Liu H. T., *Food Sci. Hum. Well.*, **2024**, *13*(4), 2208—2220
[11] Su X. M., Wang Y. Q., Bu L. Z., Zhang X., Li Y. N., Sang J. C., Ren G. M., Wen M. H., *Chem. Res. Chinese Universities*, **2025**, *41*(4), 919—928
[12] Wang L. B., Li L. Y., Gao J. Y., Huang J., Yang Y., Xu Y. Q., Liu S., Yu W. Q., *Carbohyd. Polym.*, **2021**, *260*, 117796
[13] Han X., Zhou Q., Gao Z., Lin X., Zhou K. X., Cheng X. L., Chitrakar B., Chen H., Zhao W., *Food Res. Int.*, **2022**, *162*, 112022
[14] Wu D. T., Yuan Q., Guo H., Fu Y., Li F., Wang S. P., Gan R. Y., *Food Res. Int.*, **2021**, *141*, 109888
[15] Xiao R. M., Liao W. C., Luo G. J., Qin Z. N., Han S. Y., Lin Y., *ACS Omega*, **2021**, *6*(39), 25486—25496
[16] Jeong J. H., Hong G. L., Jeong Y. G., Lee N. S., Kim D. K., Park J. Y., Park M., Kim H. M., Kim Y. E., Yoo Y. C., Han S. Y., *Curr. Issues Mol. Biol.*, **2023**, *45*(8), 6775—6789
[17] Liu T. L., Zhang M. J., Niu H. Y., Liu J., Ma R. L., Wang Y., Xiao Y. F., Xiao Z. B., Sun J. J., Dong Y., Liu X. L., *Int. J. Biol. Macromol.*, **2019**, *126*, 179—186
[18] Wang L. Y., Li K., Cui Y. D., Peng H. H., Hu Y., Zhu Z. Y., *Food Res. Int.*, **2023**, *163*, 112146
[19] Zhao H., Liu J. Y., Wang Y. Y., Shao M. T., Wang L. H., Tang W. W., Wang Y. L., Li X. L., *J. Sci. Food Agr.*, **2023**, *103*(12), 6005—6016
[20] Su S. Y., Li X. Y., Guo X., Zhou R. M., Li M. M., Ming P. F., Huang Y. Y., Rahman S. U., Ding H. Y., Feng S. B., Li J. C., Wang X. C., Li Y., Wu J. J., *Chem. Res. Chinese Universities*, **2019**, *35*(6), 1105—1110
[21] Lu N., Tan G. J., Tan H. L., Zhang X., Lv Y. L., Song X. J., You D. F., Gao Z. Y., *BioMed Res. Int.*, **2022**, *2022*, 4243210
[22] Zhang S. K., He Z. Y., Cheng Y., Xu F. Z., Cheng X. X., Wu P., *Carbohyd. Polym.*, **2021**, *260*, 117824
[23] Long X., Xie J., Xue B., Li X. H., Sun T., *J. Mol. Struct.*, **2022**, *1262*, 133047
[24] Wang L., Mao Y. G., Zeng X., Liu N., Niu C. F., Li X. X., Ma B. J., Guo L. P., Yang X. L., *Front. Nutr.*, **2022**, *9*, 877871
[25] Li X., Wang X. H., Dong Y., Song R. L., Wei J., Yu A. X., Fan Q. Q., Yao J. L., Shan D. J., Lv F., Zhong X. J., She G. M., *Ind. Crop. Prod.*, **2022**, *175*, 114288

[26] Zhang W. N., Su R. N., Gong L. L., Yang W. W., Chen J., Yang R., Wang Y., Pan W. J., Lu Y. M., Chen Y., *Carbohyd. Polym.*, **2019**, *209*, 363—371
[27] Yuan Q. X., Zhang J., Xiao C. L., Harqin C. G., Ma M. Y., Long T., Li Z. H., Yang Y. L., Liu J. K., Zhao L. Y., *Carbohyd. Polym.*, **2020**, *236*, 116047
[28] Bai Y. J., Jia X. C., Huang F., Zhang R. F., Dong L. H., Liu L., Zhang M. W., *Carbohyd. Polym.*, **2020**, *246*, 116532
[29] Ji C. F., Zhang Z. Y., Zhang B. H., Chen J. R., Liu R. Y., Song D. X., Li W. L., Lin N., Zou X., Wang J., Guo S. D., *Carbohyd. Polym.*, **2021**, *257*, 117605
[30] Wang Y. L., Han J., Yue Y., Wu Y. Z., Zhang W. Q., Xia W., Wu M. Q., *Int. J. Biol. Macromol.*, **2023**, *237*, 124142
[31] Pu X. Y., Ma X. L., Liu L., Ren J., Li H. B., Li X. Y., Yu S., Zhang W. J., Fan W. B., *Carbohyd. Polym.*, **2016**, *137*, 154—164
[32] Cao J. J., Lv Q. Q., Zhang B., Chen H. Q., *Carbohyd. Polym.*, **2019**, *212*, 89—101
[33] Liu Y. T., Duan X. Y., Zhang M. Y., Li C., Zhang Z. Q., Hu B., Liu A. P., Li Q., Chen H., Tang Z. Z., Wu W. J., Chen D. W., *Ind. Crop. Prod.*, **2021**, *159*, 113079
[34] Lai Y., Deng H. L., Chen M. Y., Fan C. H., Chen Y., Wang F., Zhou Q., Song C., *J. Food Meas. Charact.*, **2023**, *17*(5), 5506—5517
[35] Yang Y. H., Lu M. M., Xu Y. C., Qian J., Le G. W., Xie Y. L., *J. Agr. Food Chem.*, **2022**, *70*(48), 15225—15243
[36] Kong Q. H., Zhang R. F., You L. J., Ma Y. X., Liao L., Pedisić S., *Food Chem. Toxicol.*, **2021**, *151*, 112145
[37] Xu Z. P., Zhang J. J., Wu J. N., Yang S. Z., Li Y. Y., Wu Y. Y., Li S. Y., Zhang X., Zuo W., Lian X., Lin J. J., Jiang Y. S., Xie L. T., Liu Y. L., Wang P., *Front. Neurosci. Switz.*, **2022**, *16*, 976358
[38] Zhu Y. Q., Chen B. R., Zhang X. Y., Akbar M. T., Wu T., Zhang Y. Y., Zhi L., Shen Q., *Nutrients*, **2024**, *16*(16), 2660
[39] Friedland R. P., Chapman M. R., *PLOS Pathog.*, **2017**, *13*(12), e1006654
[40] Zhu G. S., Guo M., Zhao J. X., Zhang H., Wang G., Chen W., *Nutrients*, **2022**, *14*(4), 735.
[41] Kim H. W., Kim S. M., Park S. J., Park G., Shin H., Park M. S., Kim J., *Front. Aging Neurosci.*, **2021**, *13*, 709091
[42] Keung W. S., Zhang W. H., Luo H. Y., Chan K. C., Chan Y. M., Xu J., *Carbohyd. Polym.*, **2025**, *352*, 123209
[43] Sun Z., Zeng Z., Chen L. X., Xu J. D., Zhou J., Kong M., Shen H., Mao Q., Wu C.Y., Long F., Zhou S. S., Li S. L., *J. Ethnopharmacol.*, **2025**, *337*, 118958
[44] Guo B. B., Zhang W. H., Zhang J. Y., Zou J. W., Dong N. N., Liu B., *Food Res. Int.*, **2025**, *199*, 115385
[45] Wang S. Q., Yang X. M., Hou X. N., Zhu Z. Y., *Process Biochem.*, **2022**, *122*, 272—281
[46] Govindan S., Jayabal A., Shanmugam J., Ramani P., *Food Sci. Hum. Well.*, **2021**, *10*(4), 523—535
[47] Zhan X. H., Hakoupian M., Jin L. W., Sharp F. R., *Front. Aging Neurosci.*, **2021**, *13*, 7055934
[48] Yang R. L., Zhu F., Mo W. Y., Li H. L., Zhu D. L., He Z. Y., Ma X. J., *Foods*, **2024**, *13*(19), 3177
[49] Hu D. W., Bao T., Lu Y., Su H. M., Ke H. H., Chen W., *J. Agr. Food Chem.*, **2019**, *68*(46), 13016—13024
[50] Meng H. H., Wu J. J., Shen L., Chen G. W., Jin L., Yan M. X., Wan H. T., He Y., *Int. J. Biol. Macromol.*, **2022**, *215*, 398—412

(Ed.: L, V, K)